



Mechanical reliability analysis of flexible power cables for marine energy

Downloaded from: <https://research.chalmers.se>, 2025-12-04 23:39 UTC

Citation for the original published paper (version of record):

Johannesson, P., Lang, X., Johnson, E. et al (2022). Mechanical reliability analysis of flexible power cables for marine energy. *Journal of Marine Science and Engineering*, 10(6): 1-
<http://dx.doi.org/10.3390/jmse10060716>

N.B. When citing this work, cite the original published paper.

Article

Mechanical Reliability Analysis of Flexible Power Cables for Marine Energy

Pär Johannesson ¹, Xiao Lang ², Erland Johnson ^{2,3} and Jonas W. Ringsberg ^{2,*}

¹ Division of Materials and Production, Department of Chemistry and Applied Mechanics, RISE Research Institutes of Sweden, 412 79 Gothenburg, Sweden; par.johannesson@ri.se

² Division of Marine Technology, Department of Mechanics and Maritime Sciences, Chalmers University of Technology, 412 96 Gothenburg, Sweden; xiao.lang@chalmers.se (X.L.); erland.johnson@ri.se (E.J.)

³ Division of Materials and Production, Department of Chemistry and Applied Mechanics, RISE Research Institutes of Sweden, 501 15 Borås, Sweden

* Correspondence: jonas.ringsberg@chalmers.se; Tel.: +46-(0)31-7721489

Abstract: Marine power cables connected to moving devices at sea may experience millions of load cycles per year, and thus they need to be flexible due to the movements of the cable and designed for mechanical loads. In this study, the focus is on the mechanical life of flexible low- and medium voltage power cables connecting devices to hubs. The reliability design method Variational Mode and Effect Analysis (VMEA) is applied, based on identifying and quantifying different types of uncertainty sources, including scatter, model and statistical uncertainties. It implements a load–strength approach that combines numerical simulations to assess the loads on the cable and experimental tests to assess the strength of the cable. The VMEA method is demonstrated for an evaluation of bending fatigue, and is found to be a useful tool to evaluate uncertainties in fatigue life for WEC (Wave Energy Converter) system cables during the design phase. The results give a firm foundation for the evaluation of safety against fatigue and are also helpful for identifying weak spots in the reliability assessment, thereby motivating actions in the improvement process. Uncertainties in terms of scatter, statistical uncertainty and model uncertainty are evaluated with respect to the WaveEL 3.0, a WEC designed by the company Waves4Power, and deployed in Runde, Norway. A major contribution to the overall uncertainty is found to originate from the fatigue life model, both in terms of scatter and model uncertainty.

Keywords: experimental test; fatigue life; numerical simulation; power cable; reliability; uncertainty; VMEA (Variation Mode and Effect Analysis); wave energy



Citation: Johannesson, P.; Lang, X.; Johnson, E.; Ringsberg, J.W. Mechanical Reliability Analysis of Flexible Power Cables for Marine Energy. *J. Mar. Sci. Eng.* **2022**, *10*, 716. <https://doi.org/10.3390/jmse10060716>

Academic Editor: Fuping Gao

Received: 9 May 2022

Accepted: 22 May 2022

Published: 24 May 2022

Publisher's Note: MDPI stays neutral with regard to jurisdictional claims in published maps and institutional affiliations.



Copyright: © 2022 by the authors. Licensee MDPI, Basel, Switzerland. This article is an open access article distributed under the terms and conditions of the Creative Commons Attribution (CC BY) license (<https://creativecommons.org/licenses/by/4.0/>).

1. Introduction

The increased focus on sustainable energy production is a driving force for marine area energy utilization, including offshore wind, wave energy, and tidal energy. The major use of marine power cables has shifted from supplying power to isolated offshore facilities, towards the connection of offshore array systems with a broader field for utilization [1]. There are concerns related to the reliability and long-term serviceability of marine cables [2–5]. Examples of application areas include connecting grids internationally [6] and interconnecting wind turbine generators in offshore wind farms. In the current investigation the focus is on low-voltage power cables for wave energy converters (WECs), which can extract energy from waves. To increase their economic viability, WECs are designed to be grouped into arrays to maximize energy production [7], and power cables transfer the energy from the WECs to a central hub, from which it is then transmitted ashore.

The freely hanging dynamic cables used for WECs are flexible in bending and torsion, with low stiffness properties to cope with the dynamic loads, while the axial stiffness must be designed to handle large axial tension loads. The structural integrity of the flexible power cable is influenced by fatigue damage caused by fluctuating loads due to motions of the

WEC and the hub, and also due to direct loads along the cable caused by the environmental waves, currents, and wind. In view of cost-effectiveness, reliable fatigue life predictions for the cable are essential. The typical flexible power cable consists of several layers combined in a cylindrical or a helical configuration, which leads to complex mechanical behavior [8]. The analyses must include the whole wave energy system, including all mechanical couplings, to consider all these mechanical loads.

Previous research has developed a numerical approach to analyze mechanical loads and fatigue life [9]. It has also presented valuable data on cable curvature under real environmental conditions in the petroleum industry [10]. However, relevant field experiences in marine renewable energy are lacking. There is a need to develop a methodology to enhance the reliability and fatigue life assessment process of flexible power cables for WECs.

Failure Mode and Effect Analysis (FMEA) is often used in industry to achieve reliable mechanical systems and components design [11]. FMEA focuses on identifying and eliminating known or potential failures. However, it is a qualitative method, and it does not measure the resulting reliability. The failure modes are most often triggered by unwanted variation [12], thus a general design philosophy has been developed, including all different sources of unavoidable variation. This reliability and robust design methodology, called Variation Mode and Effect Analysis (VMEA), was first presented in [13,14] and was further developed in [15–17]. A more general presentation of the methodology is found in [18–22]. The VMEA method concept takes into account quantitative measures of failure causes. The method is based on statistics, reliability, and robust design, which can guide engineers to identify critical areas of unwanted variation. The technique has been successfully implemented for fatigue design and maintenance in the automotive and aeronautic industries [16,17], as well as in the marine energy field [22–24]. A main uncertainty in failure analysis of WECs is the shortage of knowledge and experiment data [9], which makes assessment design difficult. An effective reliability method must thus be able to take “lack of experience” into account. The VMEA method can combine different types of uncertainties and is applied in this study addressing the fatigue design of flexible power cables.

The flexible power cable used in this study is a low-voltage power cable mounted on the full-scale floating point-absorber WEC prototype WaveEL 3.0, developed by the company Waves4Power, see [25] for details. The WaveEL 3.0 has been deployed in Runde, Norway; see Figure 1 (right). An illustration of the WaveEL 3.0 system installation is shown in Figure 1 (left). The mooring system consists of three mooring legs. Each mooring leg has two segments connected by a submerged floater. Gravity anchors are used to fix the WEC to the seabed. The cable is freely hanging and transfers power from the WEC to a hub. The WEC and the hub are both equipped with bend restrictors to protect the cable from large bending movements of loads that may cause deformation and clashing [26]. The design service life of the WEC system is over 25 years.

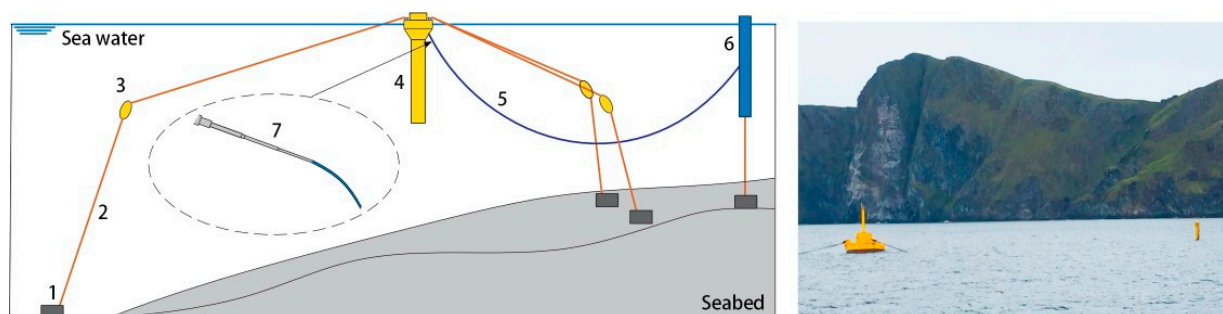


Figure 1. (Left) Illustration of the WaveEL 3.0 installation in Runde: (1) gravity anchor, (2) segment of a mooring line, (3) floater, (4) WEC, (5) cable, (6) hub, (7) bending restrictor, and (right) the full-scale WaveEL 3.0 system (photograph taken by the fourth author).

The life and ageing of cables mainly depend on chemical, electrical, and mechanical properties, and degradation. Cable manufacturers typically perform life testing and evaluation giving attention to chemical and electrical degradation [26]. The focus of this study is the fatigue life of dynamic cables subjected to repeated load cycles. The work aims to adapt and apply the VMEA methodology to quantify all uncertainty sources for life predictions of cables used in WEC array systems. Experimental tests and numerical simulations are used for quantification, and the method is demonstrated with an evaluation of bending fatigue life.

The next section introduces methodologies for numerical simulation of cable motion, fatigue life, and VMEA. The VMEA analysis results of the fatigue damage evaluation are presented in the third section, including the fatigue life model of the cable, the analysis of its uncertainties, the numerical simulation model, and the sensitivity of cable properties. A discussion and the conclusions close the paper.

2. Methodology

In this study of wave energy application, the focus is on cable fatigue life due to mechanical loads. The dynamic cable was subjected to repeated load cycles with varying bending, tension, and rotation loads, resulting in mechanical stress histories. The fatigue calculation followed the typical life evaluation process for wave energy converters cable [27]. It involved the input of marine loads, numerical simulation of WECs system, and the fatigue life model; see Figure 2. The dominant failure mode was altered according to the different platforms, cables and locations. Initial modelling of the dynamic cable and the surrounding system indicated that the bending load dominated this study. Thus, the most critical failure mode for the mechanical life of the dynamic cable was assumed to be caused by the bending loads on the cable.

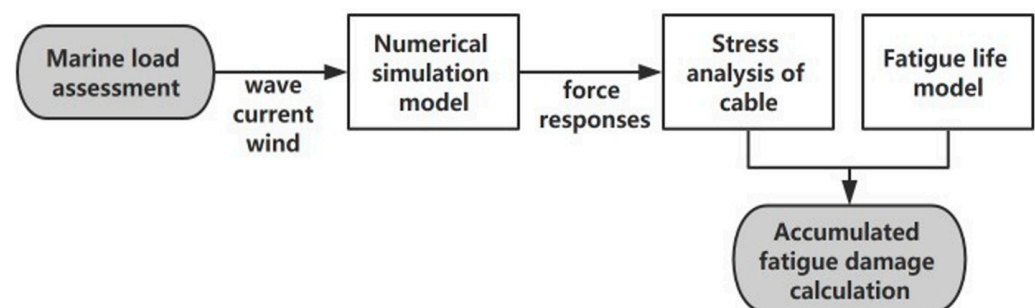


Figure 2. The typical life evaluation process for a wave energy converter cable.

The study has an emphasis on models used in numerical simulations, fatigue analysis and statistical assessment. The models used in the numerical simulations of the WEC system, and for fatigue damage calculation of the cable, have been validated in previous research work by the authors. Section 2.1 presents a brief overview of these studies, followed by a description of each model in Figure 2 in Sections 2.2–2.4.

2.1. Full-Scale Measurements on WaveEL 3.0 and Power Cable Fatigue Tests

The design of a numerical simulation model of a WEC system such as WaveEL 3.0 requires an understanding of the physics that can be represented by commercial software, in order to accurately capture the real physics ultimately affecting the motion responses of the WEC and its components, and the force responses in e.g., the power cable and the mooring lines. The simulation procedure (including the numerical simulation models) in this study was validated against WEC model tests (on a WEC system similar to WaveEL 3.0) carried out in model scale in a laboratory ocean basin [25,27]. There are, however, scaling effects that need to be considered between model and full scale. The representation and modelling of environmental loads (e.g., wave, wind, and ocean current) at full scale are also more challenging compared to model test conditions.

Ringsberg et al. [28] presented results from a full-scale measurement campaign on Waves4Power's WaveEL 3.0 WEC, deployed at a test site off the coast of Runde, Norway. The measurement campaign lasted from June to November 2017. The WEC system was instrumented with several sensors and equipment that recorded several factors, such as the WEC's motions and position, axial forces in the mooring lines, the power performance of the WEC, and the responses of the power cable from the WEC to the power-collecting hub; see Figure 1. The authors designed a simulation model of this WEC system, based on the simulation procedure validated in [25,27] and presented a comparison between the full-scale measurements and the numerical simulations regarding WEC motions and mooring-line forces. It was found that the measured and simulated WEC motion responses were in good agreement, as were the measured and simulated axial forces in the mooring lines. The numerical simulation results of the mooring-line forces were mostly 10% higher than the measurements, which was within an acceptable range of error due to uncertainties in system instrumentation, environmental conditions and tidal influence that changed the pre-tension force of the mooring lines. Therefore, the predictability of the numerical simulation model of WaveEL 3.0 was found to be good.

As part of the measurement campaign, the motions in a short segment of the power cable were recorded. Unfortunately, the resolution of the recorded data was not sufficient to compare with the results from the numerical simulation model. Nevertheless, it was possible to see that it was subjected to repeated motions resulting in load cycles with varying bending, tension, and rotation loads, resulting in mechanical stress histories that fatigue the power cable. According to [26], for wave energy applications with a power cable between the buoy and the hub, the cyclic variation of axial and bending stresses is the essential cause of the power cable's fatigue damage, where the bending stress often dominates the cyclic total stress.

A test rig generating a rotating-bending cyclic load was developed to simulate a large number of load cycles for the cable in a short time; see the test setup illustrated in Figure 3. The cable was subjected to a rotational cycle at the lower end A attached to a rail, while the upper end B of the cable was fixed. When the rail rotated around a vertical axis through point B, end A was rotated one turn back around the horizontal axis by utilizing a mechanical drive to avoid torque along the cable. This design allowed the required measurements of conductivity to be performed during testing. The cable was bent 90° . The rig permitted the radius R to be mechanically adjusted in the interval from 400 to 800 mm, defined as the distance from the connection point to the intersection point as Figure 3 shows. The test rig was set to operate at a frequency of about 2 Hz because of the internal heating limitation. The interruption criterion was interpreted as either survival after a large number of cycles which was considered as run-out, or when a failure criterion was achieved. The run-out level was decided to be 8,600,000 cycles, while an increase in electrical resistance of 15% was stated as the failure criterion. Electrical resistance was calculated by the voltage drop at a fixed electrical current, at this voltage drop many of the copper threads should have failed due to fatigue.

A numerical simulation model of the test rig was presented in [29]. It presented a methodology for modelling umbilical power cables, which was verified against a benchmark study in the literature. In the same study, the power cable used in the current study was used in the numerical model of the test rig setup. A comparison of results from the real fatigue tests verified the numerical models of the test rig and the power cable. To summarize, the numerical simulation model of the WEC system used in the study was validated in model scale in [25,27], verified against a full-scale installation in [28], and the numerical model of the dynamic power cable was verified in [29].

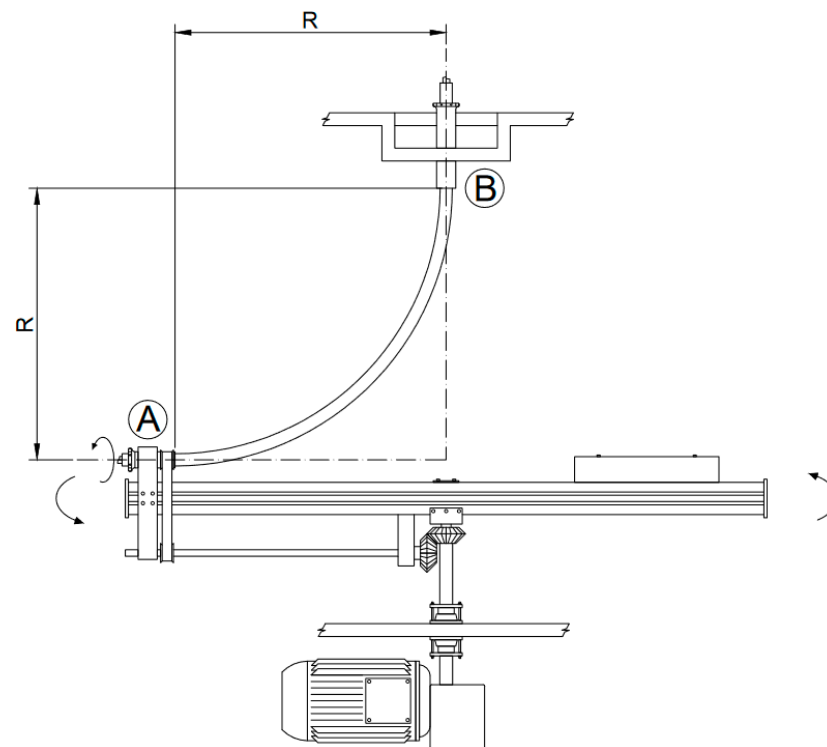


Figure 3. The test rig setup with cable mounted. The cable is fixed at the top, and the rotating end is controlled via a mechanical drive visible at the bottom of the picture (A and B are end points, see the text for clarification).

2.2. Numerical Simulation of Cable Motion

The numerical model of WaveEL 3.0 was used in the simulations, with the commercial software package DNV GL SESAM [30,31]. Due to the coupling between the components of the WEC system, the time-domain coupled simulation procedure was adopted to solve the motions of all components in the WEC system simultaneously, considering the interactions between the WEC buoy, the mooring lines, and the power cable. The coupled simulation model was developed and adapted to the Runde test-site conditions and installation [25,28].

2.3. Fatigue Life Model

A fatigue model evaluates fatigue tests and performs damage calculation for simulated loads. In this study, a Basquin-like relation was considered in conjunction with the linear Miner rule for damage accumulation; cycle amplitudes were resolved using the rainflow method. This provides a conservative damage calculation compared to using, for example, fatigue limit or the Haibach approach. In the fatigue life model, the number of cycles to failure N is related to the stress amplitude S following the Basquin equation:

$$N = N_0 \cdot \left(\frac{S}{S_0} \right)^{-m}, \quad (1)$$

where S_0 represents the fatigue strength (in terms of stress amplitude) at N_0 cycles, here selected as $N_0 = 1 \times 10^6$.

2.4. Variation Mode and Effect Analysis

VMEA is a probabilistic method that studies the variation and uncertainty around a nominal design, and an adaption to marine energy applications is found in [22]. Based on all variation and uncertainty sources, the methodology determines a statistically based safety factor that, together with an optional additional safety factor based on engineering risk judgments, gives an overall safety factor against eventual failure. The statistical safety

factor is constructed through a confidence interval, which is determined from an overall standard deviation of the defined target function. The standard deviation is generally obtained from the square root of overall variance, which can be calculated using Gauss's approximation formula. It gives the variance of the target function f as the sum of variance contributions from different influencing variables x_i , each described by its variance together with its influence of the target, employing its sensitivity coefficient c_i ; see Equation (2).

$$\text{Var}[f(x_1, x_2, \dots, x_n)] \approx \sum_{i=1}^n c_i^2 \text{Var}[x_i] + \text{Cov} \quad (2)$$

where the last term is the covariances between the influencing variables. The covariances need to be included when relevant, however, in most cases they can be neglected or be avoided by a re-parametrization of the model. This probabilistic approach represents a first-order, second-moment reliability method.

The VMEA method progresses through three different design phases; see Figure 4. The first and crudest approximation is called the “basic” VMEA, and is used in the early design phase when little is known about variations. The standard deviations and sensitivity coefficients are simply replaced by scores, on a scale from 1 to 10, based on engineering judgments about uncertainty and sensitivity, respectively. The refinement process in the next design phase is named “enhanced” VMEA. The uncertainties are quantified by judging standard deviations via standard rules, while fundamental physical knowledge is used to assess sensitivities. Further refinement in the later detailed design phase, called “probabilistic” VMEA, is developed by obtaining more information about the most critical uncertainty sources. More detailed empirical results are used to obtain the standard deviations, and sensitivity coefficients are taken from numerical sensitivity studies or differentiation of physical, mathematical models. This analysis gives an estimate of the resulting total uncertainty, and a corresponding statistical safety factor can be derived. Further, the VMEA work process is grouped into four activities: “Define-Analyse-Evaluate-Improve”, and can be described by seven steps, as illustrated in Figure 5.

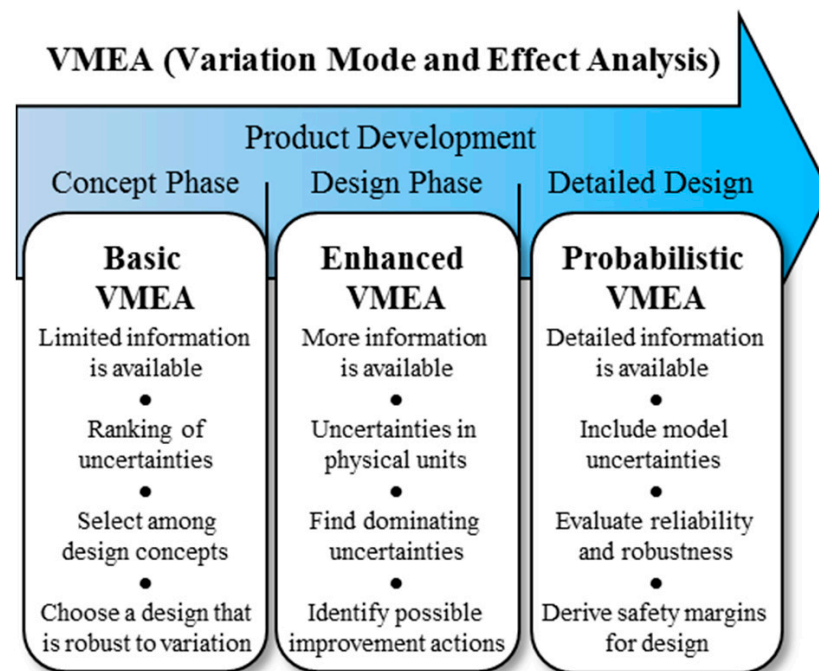


Figure 4. VMEA in different design stages.

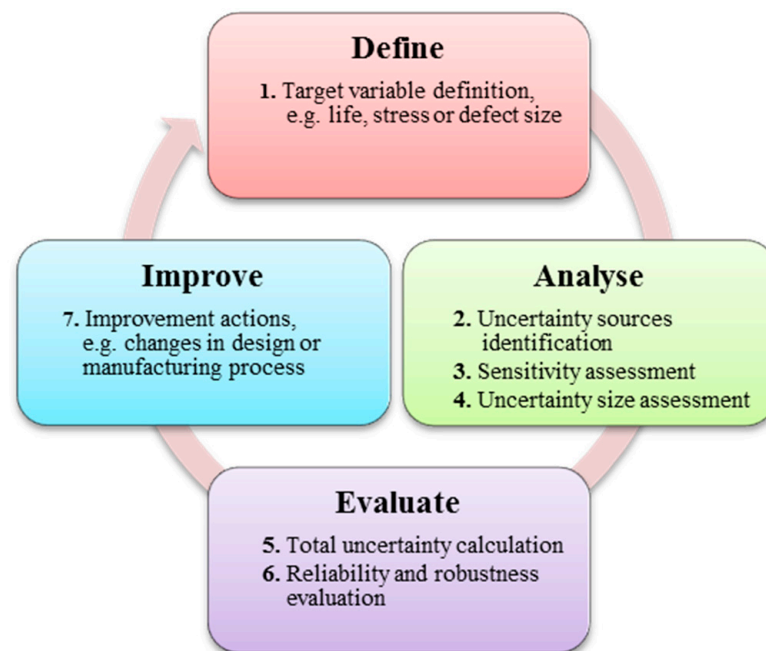


Figure 5. VMEA in the design and improvement cycle.

3. Results

First, the target variable and sources of uncertainties were identified within the basic VMEA. The results from the basic VMEA were then used as a starting point to establish a full probabilistic VMEA. The probabilistic VMEA was based on probabilistic descriptions of equivalent strength and equivalent load on the cable. These were first derived, based on the same methods as described in [17–22,24], but adapted to the current application on dynamic cables. Experimental tests of cable bending life tests were used to assess the equivalent strength, and the equivalent load was assessed using numerical cable simulation and subsequent fatigue damage calculations. The fatigue strength was evaluated from rotating bending fatigue tests, and sensitivities to parameters were investigated by numerical simulation, which was used in the probabilistic VMEA. Finally, a reliability evaluation was performed. All results are presented below.

3.1. Target Variable and Sources of Uncertainties

A basic VMEA was established, following the procedure in Figure 5, with the involvement of a cross-functional team of experts with different views and competencies within cable manufacturing, mechanics, numerical simulations, laboratory testing, and statistics. The main objective of this activity was to define the target variable and to identify sources of uncertainties.

The target variable in this study was chosen as the fatigue life of the flexible power cable. Following the life evaluation process shown in Figure 2, the uncertain sources within the cable fatigue life calculation were divided into five categories: marine load, cable motion, cable properties, fatigue life model, and laboratory testing; see the Ishikawa diagram [32] in Figure 6. The waves and the ocean currents were the two main marine loads. The WEC system and the cable were sensitive to the induced motions. The boundary conditions representing the cable connections to the buoy and the hub were modelled but exhibited uncertainties, as did the influence of marine growth. There are a few cable property parameters in the simulation model whose values affect the fatigue life. The main parameters considered are the outer diameter of the cable, the mass per meter, and stiffnesses in axial, bending and torsional directions.

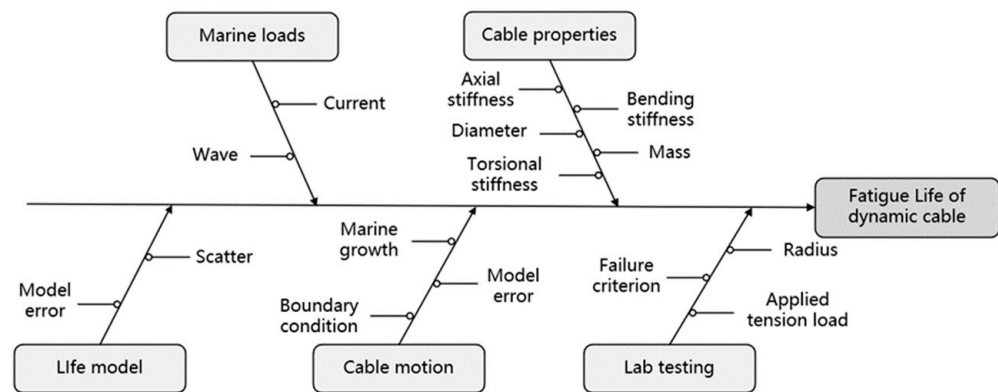


Figure 6. Ishikawa diagram [32] for the given uncertainty sources for the VMEA application of flexible power cable reliability and fatigue assessment process design.

A random variation in fatigue life and other uncertainties exist due to estimation of the life model and possible model errors in the fatigue life model. Several potential uncertainty sources were present in the laboratory testing due to the boundary conditions in the cable's attachment in the test rig, the evaluation of the failure criterium in terms of conductivity drop, the cable bending radius, and the applied axial load that should be zero. The influence of stress from a possible unwanted axial load in the test rig should be negligible compared to the contribution of the bending load.

3.2. Equivalent Load and Strength Variables

The load and strength variables were defined as stress amplitudes measured in unit MPa based on fatigue equivalent load and strength amplitudes corresponding to N_{eq} number of cycles, here chosen to $N_{eq} = 1 \times 10^6$ cycles. The choice of equivalent number of cycles is arbitrary, but was chosen to acquire meaningful interpretations of the equivalent load and strength variables. The equivalent load, L_{eq} , is defined as the fatigue equivalent stress amplitude at N_{eq} cycles corresponding to the target life, T_{life} , which is chosen to $T_{life} = 25$ years in this study. The equivalent strength, S_{eq} , is defined as the stress amplitude in the Wöhler curve at N_{eq} cycles to failure. Note that the equivalent load and strength variables are connected through the same equivalent number of cycles, $N_{eq} = 1 \times 10^6$, together with the damage exponent of the Wöhler curve, chosen to $m = 6.236$, which is the value from [8], also used in [26]. It can be observed that the parameters for the bending stiffness, EI , and the cable diameter, d , are common for equivalent load and strength definitions. The target variable Y is defined as the difference between the logarithmic strength and load, namely $Y = \ln(S_{eq}) - \ln(L_{eq})$.

The strength of the cable was investigated experimentally by life testing at different bending radii on the cable. The results were modelled by a life–strength relation following the Basquin Equation (1), where the number of cycles to failure N were related to the bending curvature k :

$$N = N_0 \cdot \left(\frac{k}{k_0} \right)^{-m}, \quad (3)$$

where k_0 represents the fatigue strength (in terms of the curvature of cable) at $N_0 = 1 \times 10^6$ number of cycles.

For the VMEA, strength and load measures were compared, requiring a common dimension, here chosen as stress. Pure bending was considered, employing beam theory to relate the curvature to maximum stress S according to:

$$S = \frac{32EI}{\pi d^3} \cdot k \quad (4)$$

with d being the diameter and EI the bending stiffness of the cable.

Assuming a fixed damage exponent m , using Equation (3), each observed life can be recalculated into a damage-equivalent curvature, $k_{eq,i}$, at N_{eq} cycles, and the logarithmic mean estimated from the fatigue tests as:

$$\ln k_{eq} = \frac{1}{n} \sum_{i=1}^n \ln(k_{eq,i}), \quad k_{eq,i} = k_i \cdot \left(\frac{N_i}{N_{eq}} \right)^{\frac{1}{m}} \quad (5)$$

with N_i being the observed life at the curvature k_i . Defining the equivalent stress S_{eq} as the stress amplitude in the Wöhler curve that corresponds to N_{eq} cycles to failure, as Equation (4) gives:

$$S_{eq} = \frac{32EI}{\pi d^3} \cdot k_{eq} \quad (6)$$

The estimated Wöhler curve for the fatigue bending tests are presented in Figure 7. The equivalent curvature was estimated to $k_{eq} = 1.64 \text{ m}^{-1}$, using Equation (5) with exponent $m = 6.236$, which is consistent with the test data illustrated in Figure 7. The nominal value of the equivalent strength was then estimated to $S_{eq,nom} = 1.41 \text{ MPa}$, using Equation (6). Additional tests would be beneficial to obtain additional valuable knowledge. However, the limited amount of data is reflected in the uncertainty size assessment as demonstrated below.

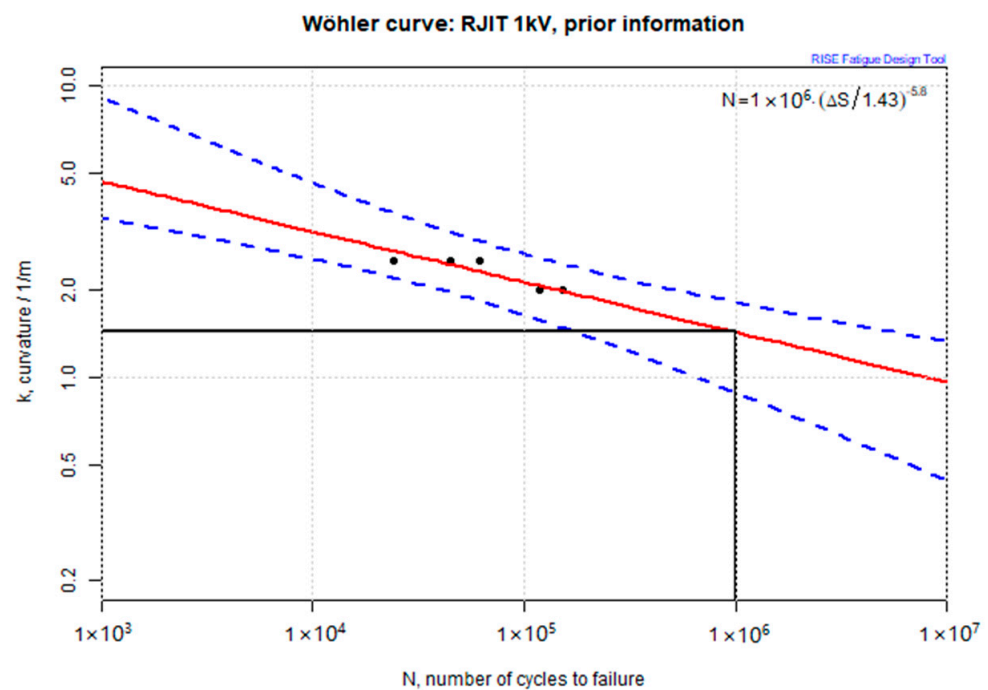


Figure 7. Estimated Wöhler curve of the cable, using prior knowledge on the exponent m , where the circles are experimental data, the solid line is the estimated Wöhler curve, and the dashed lines the 95% confidence intervals.

In parallel, a corresponding equivalent load is needed. In the simulations, the fatigue damage was calculated based on the wave climate at Runde, defined by the wave scatter diagram. The calculations were performed as follows. The wave scatter diagram is defined by the matrix $F = (f_{ij})$, where the indices represent the significant wave height, $H_{s,i}$, and the wave period, $T_{p,j}$, and these are discretized in steps. The matrix position f_{ij} specifies the number of hours that each sea state occurs during one year. For each sea state $(H_{s,i}, T_{p,j})$, the cable was simulated for one hour using the finite element method, and the

accumulated fatigue damage D_{ij} calculated using the Palmgren-Miner rule, the rainflow counting method, and the S-N-curve, Equation (1), according to:

$$D_{ij} = \sum_k \frac{n_k}{N(L_k)} = \sum_k \frac{n_k}{N_0} \left(\frac{L_k}{S_0} \right)^m = \frac{1}{N_0 S_0^m} \sum_k n_k L_k^m = \frac{1}{N_0 S_0^m} d_{ij} \quad (7)$$

where n_k is the number of stress cycles with amplitude L_k , and d_{ij} is the so-called pseudo damage for one hour. The total damage for one year can now be calculated as:

$$D_1 = \sum_{i,j} f_{ij} \cdot D_{ij} = \frac{1}{N_0 S_0^m} \sum_{i,j} f_{ij} \cdot d_{ij} = \frac{d_1}{N_0 S_0^m} \quad (8)$$

Note that d_1 , the total pseudo damage for one year, only depends on the simulated load and parameter m , but not on the fatigue strength S_0 . The most critical position along the cable with the maximum damage value is chosen. The fatigue damage corresponding to the target life T_{target} becomes:

$$D_{target} = D_1 \cdot T_{target} \quad (9)$$

We now introduce the equivalent load L_{eq} as the stress amplitude that, for N_{eq} cycles, gives the same fatigue damage during the target life as D_{target} , and by using the Basquin equation in Equation (1), the equivalent damage is calculated as:

$$D_{eq} = \frac{N_{eq}}{N_0 \cdot \left(\frac{L_{eq}}{S_0} \right)^{-m}} = \frac{N_{eq} L_{eq}^m}{N_0 S_0^m} \quad (10)$$

Consequently, by solving $D_{target} = D_{eq}$, the equivalent load is calculated according to:

$$L_{eq} = \left(\frac{d_1 \cdot T_{target}}{N_{eq}} \right)^{\frac{1}{m}} = (T_{target})^{\frac{1}{m}} \cdot L_{eq,1} \quad (11)$$

with $L_{eq,1}$ being the equivalent load for one year. Using results from numerical simulations of the motions of the cable, the nominal value of the equivalent load was estimated at $L_{eq,nom} = 0.47$ MPa, using Equation (11).

Based on the equivalent strength, S_{eq} , and the equivalent load, L_{eq} , the target function Y is defined according to:

$$Y = \ln(S_{eq}) - \ln(L_{eq}) \quad (12)$$

where negative values of Y indicate failure, while the safe region corresponds to positive values. The equivalent load, L_{eq} , the equivalent strength, S_{eq} , and the target function, Y , are stochastic variables, and their variations are due to uncertainties in their underlying dependent variables. These are investigated in the next subsection.

The logarithmic scale was chosen since experience has shown that it reduces non-linearities of the target function, thus reducing errors due to linearization of the target function. Further, the logarithmic scale makes the variance representation of uncertainty less dependent on the scale. This is taken advantage of in the VMEA analysis in the next subsection.

3.3. Evaluation of Sensitivities and Uncertainty Sizes

The probabilistic VMEA was established based on the uncertainty sources identified in the basic VMEA, and the developed models for equivalent strength and load. The variation of the target function $Y(X_1, X_2, \dots, X_p)$ depends on several uncertainty sources, X_1, X_2, \dots, X_p , where p is the number of variables. If the uncertainty sources are considered

as independent random variables, the Gauss approximation formula for the target function gives its variance as a function of the variances of each uncertainty source according to:

$$\tau^2 = \text{Var}[Y(X_1, X_2, \dots, X_p)] = \sum_{i=1}^p \left(\frac{\partial Y}{\partial X_i} \right)^2 \cdot \text{Var}[X_i] = \sum_{i=1}^p c_i^2 \cdot s_i^2 \quad (13)$$

where s_i is the standard deviation of uncertainty source X_i . The sensitivity coefficients c_i are the partial derivatives of Y with respect to X_i . The logarithmic scale of the target function in Equation (12) implies that the uncertainties represent relative standard deviations that can be judged in terms of uncertainty in percentage.

The sensitivities and sizes of the uncertainty sources judged to be of most importance in the basic VMEA were evaluated. The assessment of each uncertainty source is detailed below, and the results are summarized in a so-called VMEA table; see Table A1 in Appendix A, where the total uncertainty is also shown. The uncertainty sources were grouped in the same way as for the basic VMEA, as shown in Figure 6.

Many uncertainties must be assessed by engineering judgements. Engineers are sometimes unfamiliar with statistical properties like standard deviations, but may find it easier to make judgements about the possible uncertainty interval of a certain property. From such a judgement of an uncertainty interval of $\pm x\%$, the standard deviation of the uncertainty source can be calculated assuming a uniform distribution, namely:

$$s = \frac{x\%}{\sqrt{3}}. \quad (14)$$

The uniform distribution interpretation of an uncertainty interval has been used throughout this study, unless indicated otherwise.

3.3.1. Marine Loads

Wave climate in Runde: Based on simulations in [26], sensitivity coefficients due to marine load parameters were evaluated. Significant wave height varied between values $H_{S,1} = 1.5$ m and $H_{S,2} = 7.5$ m, and the sensitivity depended only on the load and was evaluated to $c_{H_s} = -1.31$. Experts judged the relative uncertainty in significant wave height to be around $\pm 10\%$ and consequently, assuming a uniform distribution, the uncertainty became $10\% / \sqrt{3} = 5.8\%$. Similarly, the influence of ocean current was evaluated, and the sensitivity coefficient became 0.67, and the relative uncertainty 5.8%.

3.3.2. Cable Motion

Cable boundary conditions and model error: In the simulations in [26], the boundary condition of the buoy and the hub was judged to be well modelled, and the total system was verified in [28,33]. The model error due to cable boundary conditions was judged to be at most $\pm 5\%$, which translates to an uncertainty of 2.9%, assuming a uniform distribution. The model error due to the cable motion simulation model was judged to be $\pm 10\%$, which translates to an uncertainty of 5.8%. Since these were judged to be total uncertainties in the target function, the corresponding sensitivity coefficients equal unity.

Marine growth: In the simulations, see [26] for data, different models for marine growth were assumed. The resulting uncertainty due to marine growth was estimated to 10.5%. This value was achieved by considering two extreme cases and assuming a uniform distribution between these. Since the uncertainty was evaluated with respect to the target function, the corresponding sensitivity coefficient equals unity.

3.3.3. Cable Properties

The applied and installed cable was a 1.2 kV low-voltage cable, consisting of three conductors laid together with Kevlar ropes. The outer sheathing comprised two layers of polyurethane (PUR) material.

Cable diameter: The cable diameter was 39 mm. The variation due to manufacturing was judged by production engineers as max variation intervals $\pm x$ mm. This interval was interpreted as a uniform distribution giving a standard deviation $x/\sqrt{3}$, and finally, the relative uncertainty, see Table A1 in the Appendix A for estimated values. It should be noted that for different sizes of cables, the uncertainty may vary.

The diameter of a cable impacts the load and the strength. Since the same basic cable model was used for the cable simulation (for load evaluation) and the conversion between bending radius in test and bending stress (the strength evaluation), the corresponding sensitivities due to the diameter was evaluated zero.

Cable stiffnesses: The cable stiffness parameters EI , EA and GKv were evaluated based on tests; see [28,29,34], and the corresponding uncertainties are shown in Table A1 in Appendix A for estimated values.

The parametric sensitivity analysis within a total of 27 cases with different cable bending stiffness ($EI = 2, 4, 6 \text{ Nm}^2$), axial stiffness ($EA = 2, 4, 6 \text{ MN}$) and torsion stiffness ($GKv = 1.5, 3.0, 4.5 \text{ Nm}^2/\text{rad}$) were simulated; see [26,29,34] for simulation results and stress analyses. The bending stress component was extracted from these simulations, and sensitivity coefficients for cable stiffness were assessed. A multivariate regression model was fitted to all the simulation results in the evaluation, representing a linear response surface. The sensitivities to EA and GKv were close to zero, as expected since only the bending stress was used in the evaluation. Sensitivity depends on load and strength; the equivalent strength was evaluated from the bending radius according to Equation (9). From this relation, one notes that the equivalent nominal stress depends linearly on EI but has no dependence on EA and GKv . Consequently, the strength sensitivities in log-scale become one for EI and zero for EA and GKv . The total sensitivities thus become approximately zero.

Mass of cable: Based on simulation in [26], the sensitivity coefficient due to mass was evaluated. The parameter varied from low, to medium, to high as 2 kg/m, 2.75 kg/m, and 6 kg/m.

The load sensitivity coefficient was similar to the above, defined in log-scale and where the equivalent load was calculated using Wöhler exponent $b = 6.238$. The load sensitivity coefficient was calculated to 1.52. The equivalent nominal strength does not depend on the mass of the cable, $c_M = 0 - 1.52 = -1.52$. The maximum variation of the mass was judged to $\pm 2\%$, which is interpreted as uniform distribution and giving the uncertainty $2\%/\sqrt{3} = 1.2\%$.

3.3.4. Life Model

Uncertainties due to fatigue model: The identified uncertainty sources include fatigue scatter, estimation uncertainty and fatigue model error. These influence only the strength aspect and not the load aspect of the target function.

Uncertainty due to fatigue scatter was evaluated from the fatigue tests. The standard deviation of the logarithmic equivalent curvature, $\ln(k_{eq,i})$, was evaluated to $s = 5.9\%$. The uncertainty in VMEA required adjustment by a t-correction factor, taking the limited number of tests into account, $t_{corr} = 1.4$, corresponding to 4 DOF (number of tests under consideration, 5, minus the number of estimated model parameters, 1). The resulting uncertainty due to fatigue scatter is thus $t_{corr} \cdot s = 8.3\%$. The estimation uncertainty was evaluated by the standard deviation of Equation (5), giving $t_{corr} \cdot s/\sqrt{5} = 3.7\%$. The sensitivity coefficient equals unity since the uncertainties were evaluated in terms of $\ln(S_{eq})$.

The possible model error in fatigue life, here considered as an uncertainty, was judged by experience as a factor of 2 in life, corresponding to an uncertainty of 40%, assuming a uniform distribution. From Equation (1), one observes that the stress amplitude depends on the life (number of cycles) raised to the power of $1/m$. The sensitivity coefficient with respect to logarithmic fatigue scatter and logarithmic fatigue model error thus becomes $1/m = 0.16$.

3.3.5. Laboratory Testing

Bending radius uncertainty: The description and results from the rotating-bending fatigue cable tests are presented in [29,34]. The bending radius in the test influenced the strength but not the load. Equation (4) shows that the equivalent strength is inversely proportional to the bending radius, $R = 1/k$. The logarithmic sensitivity thus becomes -1 . The uncertainty in the bending radius originated from cable mounting in the test rig and dynamic effects evaluated by simulations of the cable rig. The total uncertainty contribution was evaluated at 5%. Other possible systematic errors in the test setup are assumed to be negligible and were thus neglected. The random uncertainties due to lab testing are assumed to have been captured by the estimated scatter in fatigue.

3.4. Probabilistic VMEA Table

The results from the probabilistic VMEA table are summarized and presented in the Appendix A, Table A1. The total uncertainty of the target variable Y was estimated to $\tau = 19.4\%$, i.e., the uncertainty in the predicted life of the dynamic cable was estimated to 19.4% in terms of relative standard deviation. The total uncertainty is used below to derive safety factors for design.

Further, it can be observed that the five most considerable resulting uncertainties are due to wave climate, cable model error, marine growth, fatigue scatter, and fatigue model error. Since these uncertainty sources dominate the total uncertainty, they should be the candidates for further studies, e.g., investigating if they can be more accurately assessed or if by some measure they can be reduced.

3.5. Reliability Evaluation

The target function, also called limit state function, should exceed zero with a proper safety margin. The evaluated total uncertainty of the target function, together with nominal values of equivalent strength and load, can be used to calculate a reliability index and to derive safety factors.

First, we present safety factors derived through the Cornell reliability index, and then we introduce the concept of an extra safety factor. More details are found in [22]. Together with the total uncertainty of Y from the VMEA analysis, τ , the Cornell reliability index is defined as:

$$\beta = \frac{\ln(S_{eq,nom}) - \ln(L_{eq,nom})}{\tau} \quad (15)$$

where the nominator is the nominal difference between the logarithm of the nominal values of strength and load, respectively, and the denominator, τ , is the total uncertainty from the VMEA. For our case, the reliability index becomes:

$$\beta = \frac{0.34 - (-0.76)}{19.4\%} = 5.7 \quad (16)$$

The reliability index is denoted as the safety index or distance from failure mode, since it can be interpreted as the number of standard deviations from the failure mode [12,35].

A requirement of 95% reliability corresponds to a reliability index $\beta > \beta_{req} = 1.64$, assuming a normal distribution. This reliability level is fulfilled in the current case. Further, it can also be converted into a required safety factor:

$$SF_{95\%} = \exp(\beta_{req} \cdot \tau) = \exp(1.64 \cdot 0.194) = 1.4 \quad (17)$$

However, for an engineering design, a 95% reliability is often not sufficient. This can be addressed by increasing the required reliability index. However, knowledge about rare events, representing the tail of the statistical distribution, is often relatively weak. Instead,

the reliability model can address this problem in the following way. The required distance between logarithmic load and strength is formulated as:

$$\ln(S_{eq,nom}) - \ln(L_{eq,nom}) > \beta_{req} \cdot \tau + \delta_E \quad (18)$$

where β_{req} is related to the statistical safety and δ_E defines an extra safety distance. From this expression, a safety factor SF can be calculated according to:

$$SF = \exp(\beta_{req} \cdot \tau) \cdot \exp(\delta_E) = SF_{95\%} \cdot SF_E \quad (19)$$

The safety factor is thus subdivided into two parts. The first part, $SF_{95\%}$, representing 95% reliability, is related to the combined uncertainty of all possible uncertainty sources, and is found through the probabilistic VMEA procedure. The second extra safety factor, SF_E , is related to unknown and extreme events and estimated by engineering experience combined with judgment about the severity of the risk, i.e., the likelihood of rare detrimental events and the consequence of failure. Guidance and further details can be found in [22]. The concept of reliability evaluation using the limit state function is illustrated in Figure 8.

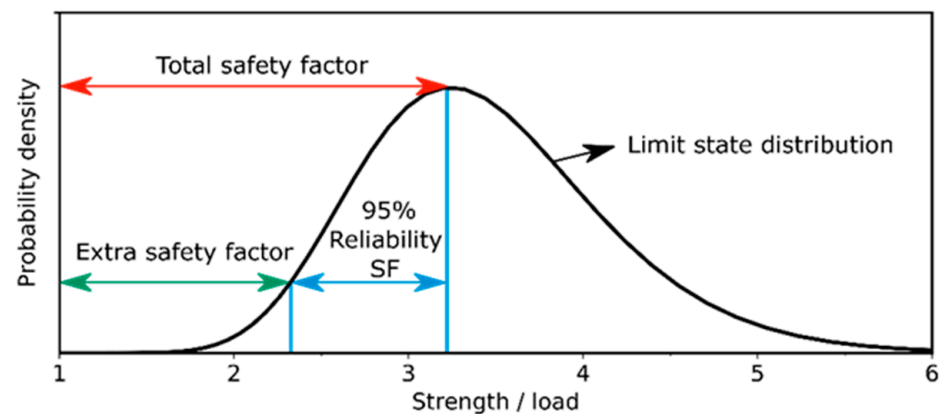


Figure 8. Load–strength limit state function.

4. Discussion of Results

The VMEA methodology has been introduced and adapted to marine cables in WEC systems. The methodology has been described in terms of a seven-step procedure, and its capacity to identify and quantify all uncertainties demonstrated. With these uncertainties as a basis, the safety against fatigue within a load–strength reliability framework has been evaluated. Uncertainties originate from different sources including scatter, model uncertainties and statistical uncertainties. A unique feature of the VMEA methodology is that it incorporates all these different sources in a unified framework. The methodology can be applied at different stages in the design process, and it has here been adapted to two different design stages, an early stage of basic VMEA with the emphasis on defining the target function and identifying the sources of uncertainty, and a later design stage of probabilistic VMEA, which has been the main part of the work.

The basic VMEA was initially performed with a group of experts with complementary perspectives, knowledge, and experiences. This group identified the sources of uncertainty relating to bending fatigue failure, and made judgements about their magnitudes and sensitivities. Based on these estimations, the respective contributions of each source to the uncertainty in the load–strength fatigue model were calculated. The uncertainty sources were grouped into five categories. The fatigue life model's uncertainty was found to contribute most to the overall uncertainty in the predicted fatigue life. These uncertainty evaluations gave important information for preparation of the more detailed probabilistic VMEA. Since the fatigue model's uncertainty was found to contribute more than other factors, in the next stage action was taken to reduce uncertainties in the fatigue model.

In the probabilistic VMEA phase, the uncertainty sources are assessed using quantitative information about uncertainties and sensitivities. These may be obtained through a combination of experimental tests, numerical simulations or mathematical relations.

For the experimental investigations, a test rig was developed for rotating cable fatigue tests, and tests were performed to evaluate cable properties including the bending fatigue strength.

A numerical simulation model of the whole WEC system was developed based on the DNV GL software package. The simulations were essential for many reasons. First, they were used to calculate the cable motion and to identify the most critical fatigue region on the cable. Simulations were also important to obtain a quantitative correction of the dynamic effects in the test rig that were not possible to measure during the live tests. By putting the marine field load conditions into the WEC system simulations, the fatigue load on the cable could be evaluated during different environmental conditions. Finally, parametric sensitivity analyses were performed with the numerical model to evaluate sensitivities for most of the uncertainty sources, including load- and strength-related sources.

For the uncertainty sources directly related to the fatigue load-strength and the fatigue life models, mathematical expressions were used directly based on simpler beam models or empirical relations, and these enabled simple calculations of the corresponding sensitivity factors.

These three different approaches were thus integrated with the VMEA methodology and the uncertainties in terms of scatter, statistical uncertainty and model uncertainty were evaluated for the different uncertainty sources. It was also demonstrated how the resulting total uncertainty can be used to calculate reliability indices, and to evaluate safety factors against fatigue failure. It should be noted that the limited amount of data (e.g., cable experimental tests and numerical simulations) is reflected by the assessed uncertainties.

A major contribution to the overall uncertainty comes from the fatigue life model, both in terms of scatter and model uncertainty. This was also the major uncertainty source identified with the basic VMEA. The second and third largest uncertainty sources switched order compared to the basic VMEA, and so did also the two least significant uncertainty sources.

The identification of the dominating uncertainty sources is useful for several reasons. The more significant uncertainty sources from a basic VMEA show where attention should be focused in the following more detailed probabilistic VMEA. It also shows where to apply focus if the uncertainty needs to be reduced.

In addition to the identification of the dominating uncertainty sources, the VMEA results also gave a basis for calculation of safety factors and reliability indices. It has been demonstrated how to derive safety factors based on the probabilistic VMEA. For a 95% reliability requirement, the load unit's safety factor became 1.4.

The connection between the safety factor and all uncertainty sources enabled the identification of the dominating uncertainties. From these, guidelines can be drawn to reduce the overall uncertainty and thereby decrease the required safety factor.

The specific cable in this study was a 1.2 kV low-voltage cable with a small diameter of 39 mm. It should be noted that other cables, including those with larger radius for higher voltage ratings, may have very different properties and different uncertainty levels. Therefore, both the relevant uncertainty sources and their sizes need to be re-evaluated for each specific case; the current study should be useful as an assessment template. Obviously, the results of this study represent not only a specific cable, but also a specific geographic location (Runde in Norway) and the specific platforms (WEC and hub of the WaveEL 3.0 prototype) used in the simulation. Thus, new numerical simulations need to be performed when investigating different set-ups. Future work should include applying the methodology to different case studies to consider the effect of changing locations, platform designs and cable designs.

5. Conclusions

A model framework has been developed for analyzing the mechanical life of flexible marine cables. It is based on the VMEA reliability design method, together with a load–strength approach that combines numerical simulations to assess load on the cable with experimental tests to assess cable strength. Experiments and calculations are also included for calculations of uncertainties and sensitivities. The main key findings and highlights from the investigation are the following:

The framework enables identification and calculations of all types of uncertainty sources, such as scatter, model uncertainties and statistical uncertainties. This is demonstrated for an evaluation of bending fatigue. The method was found to be a useful tool for evaluating uncertainties in fatigue life during the design phase. The uncertainty results gave a firm foundation for the evaluation of safety against fatigue, helpful for identifying weak spots in reliability assessment to motivate actions in the improvement process.

Specifically, the model allows the dominating uncertainty sources to be obtained, which is useful information when a reduction of overall uncertainty or an increase of safety factor is needed. The framework will be of interest for future studies of other types of wave energy systems at different locations and under different environmental conditions. However, a limitation is that for applications where only minor experience is available, it could be difficult to identify all the important uncertainty sources.

Author Contributions: The work presented in this research article engaged several researchers who had different responsibilities and contributions to the entire project, and this research article in particular. P.J. was the main contributor to the establishment of the VMEA reliability methodology, and performed the statistical analyses and the VMEA uncertainty assessment. He also contributed to the conceptualization, formal analyses, and contributed to writing main parts of the paper, reviewing and editing. X.L. carried out a significant number of numerical simulations using the SESAM software, contributed to the formal analyses, investigations, and visualization of the results. He was also responsible for the preparation of the article and writing the original draft. E.J. was deeply involved in the conceptualization and establishment of the methodology. He contributed to the statistical and formal analyses, and assisted X.L. in writing parts of the paper, reviewing and editing the final draft of the paper. J.W.R. was involved in funding acquisition and project administration. He was responsible for the supervision of X.L., and he contributed actively to the conceptualization and establishment of the methodology. He contributed to all analyses and investigations presented in the paper, including writing parts of the paper, reviewing and editing. All authors have read and agreed to the published version of the manuscript.

Funding: The research was partially funded by strategic internal funding from Chalmers University of Technology and from RISE Research Institutes of Sweden, from Chalmers University of Technology Foundation for the strategic research project “Hydro- and aerodynamics”, and by the Swedish Energy Agency projects “R&D of dynamic low voltage cables between the buoy and floating hub in a marine energy system” under contract No. 41240-1, and “Simulation model for operation and maintenance strategy of floating wave energy converters—analysis of fatigue, wear, and influence of biofouling for effective and profitable energy harvesting” under contract No. 36357-2.

Institutional Review Board Statement: Not applicable.

Informed Consent Statement: Not applicable.

Data Availability Statement: Not applicable.

Acknowledgments: The authors want to acknowledge the support from the company NKT cables (Sweden) with the delivery of cables for testing and for cooperation throughout the work. The authors also acknowledge Shun-Han Yang for her contributions to the study and the projects.

Conflicts of Interest: The authors declare no conflict of interest. The funders had no role in the design of the study, in the collection, analyses, or interpretation of data, in the writing of the manuscript, or in the decision to publish the results.

Appendix A

Table A1. Probabilistic VMEA for dynamic cable.

Input				Result	
Uncertainty Components	Sensitivity	Uncertainty	Resulting Uncertainty	Variation Contribution	
				Variance/10 ⁴	Proportion
Marine Loads					
Wave climate at site (Runde)	−1.31	5.8%	7.6%	57	15%
Ocean currents at site (Runde)	−0.67	5.8%	3.9%	15	4%
Total Marine Loads			8.5%	72	19%
Cable Motion					
Cable boundary conditions	−1.00	2.9%	2.9%	8	2%
Cable model error	−1.00	5.8%	5.8%	33	9%
Marine growth	−1.00	10.5%	10.5%	110	29%
Total Cable Motion			12.3%	152	40%
Cable Properties					
Diameter, within batch variation	0.00	0.3%	0.0%	0	0%
Diameter, batch variation	0.00	0.7%	0.0%	0	0%
Diameter, non-spherical	0.00	2.2%	0.0%	0	0%
Axial stiffness, <i>EA</i>	0.01	8.1%	0.1%	0	0%
Bending stiffness, <i>EI</i>	−0.03	12.2%	0.4%	0	0%
Torsional stiffness, <i>GK_v</i>	0.01	4.4%	0.0%	0	0%
Mass [kg/m]	−1.52	1.2%	1.8%	3	1%
Total Cable Properties			1.8%	3	1%
Life Model					
Fatigue life scatter	1	8.4%	8.4%	70	18%
Fatigue life estimation	1	3.7%	3.7%	14	4%
Fatigue life model error	0.16	40.0%	6.4%	41	11%
Total Life Model			12.9%	125	33%
Laboratory testing					
Bending radius of cable [mm]	−1.00	5.0%	5.0%	25	7%
Total Laboratory Testing			5.0%	25	7%
Total Uncertainty			19.4%	377	100%

References

1. Worzyk, T. Application of submarine power cable. In *Submarine Power Cables: Design, Installation, Repair, Environmental Aspects*, 1st ed.; Springer: Berlin, Germany, 2009; pp. 1–7. ISBN 978-3-642-01269-3.
2. DNV GL. Offshore Wind Industry Joins Forces to Reduce Costs of Cable Failures. 2018. Available online: <https://www.dnvgl.com/news/offshore-wind-industry-joins-forces-to-reduce-costs-of-cable-failures-117811> (accessed on 18 May 2022).
3. Offshore Wind Programme Board. Offshore Wind Programme Board. Export Cable Reliability Description of Concerns. Technical Report. July 2017. Available online: <https://ore.catapult.org.uk/app/uploads/2018/02/Export-Cable-Reliability-Step-1-v7-UPDATE-Jul-17.pdf> (accessed on 18 May 2022).
4. 4COffshore. Joint Industry Project Looks to Reduce Cable Failures. 2018. Available online: <https://www.4coffshore.com/news/joint-industry-project-looks-to-reduce-cable-failuresnid7457.html> (accessed on 18 May 2022).
5. Marazzato, H.; Barber, K.; Jansen, M.; Graeme, B. Cable Condition Monitoring to Improve Reliability. 2004. Available online: https://www.nexans.co.nz/NewZealand/2012/22_1.04.2004%20-%20Cable%20Condition%20Monitoring.pdf (accessed on 18 May 2022).

6. Hammons, T.J.; Woodford, D.; Loughtan, J.; Chamia, M.; Donahoe, J.; Povh, D.; Bisewski, B.; Long, W. Role of HVDC transmission in future energy development. *IEEE Power Engng. Rev.* **2000**, *20*, 10–25. [\[CrossRef\]](#)
7. Folley, M.; Whittaker, T.J.T. The effect of sub-optimal control and the spectral wave climate on the performance of wave energy converter arrays. *Appl. Ocean Res.* **2009**, *31*, 260–266. [\[CrossRef\]](#)
8. Nasution, F.P.; Sævik, S.; Gjøssteen, J.K.Ø.; Berg, S. Experimental and finite element analysis of fatigue performance of copper power conductors. *Int. J. Fatigue* **2013**, *47*, 244–258. [\[CrossRef\]](#)
9. Thies, P.R.; Johanning, L.; Smith, G.H. Assessing mechanical loading regimes and fatigue life of marine power cables in marine energy application. *Proc. Inst. Mech. Eng. Part O J. Risk Reliab.* **2011**, *226*, 18–32. [\[CrossRef\]](#)
10. Trarieux, F.; Lyons, G.J.; Patel, M.H. Investigation with bandwidth measure for fatigue assessment of the Foinaven dynamic umbilical including VIV. *Engng. Struct.* **2006**, *28*, 1671–1690. [\[CrossRef\]](#)
11. Stamatis, D.H. *Failure Mode and Effect Analysis: FMEA from Theory to Execution*, 2nd ed.; American Society for Quality, Quality Press: Milwaukee, WI, USA, 2003; pp. 21–81. ISBN 0-87389-598-3.
12. Davis, T.P. Science, engineering and statistics. *Appl. Stoch. Models Bus Ind.* **2006**, *22*, 401–430. [\[CrossRef\]](#)
13. Chakhunashvili, A.; Johansson, P.; Bergman, B. Variation mode and effect analysis. In Proceedings of the Annual Reliability and Maintainability Symposium, Los Angeles, CA, USA, 26–29 January 2004.
14. Johansson, P.; Chakhunashvili, A.; Barone, S.; Bergman, B. Variation mode and effect analysis: A practical tool for quality improvement. *Qual. Reliab. Engng. Int.* **2006**, *22*, 865–876. [\[CrossRef\]](#)
15. Chakhunashvili, A.; Barone, S.; Johansson, P.; Bergman, B. Robust product development using variation mode and effect analysis. In *Robust Design Methodology for Reliability: Exploring the Effects of Variation and Uncertainty*, 1st ed.; Bergman, B., de Mare, J., Loren, S., Svensson, T., Eds.; John Wiley & Sons Ltd.: West Sussex, UK, 2009; pp. 57–70. ISBN 978-0-470-71394-5.
16. Johansson, P.; Svensson, T.; Samuelsson, L.; Bergman, B.; de Mare, J. Variation mode and effect analysis: An application to fatigue life prediction. *Qual. Reliab. Engng. Int.* **2009**, *25*, 167–179. [\[CrossRef\]](#)
17. Svensson, T.; de Mare, J.; Johansson, P. Predictive safety index for variable amplitude fatigue life. In *Robust Design Methodology for Reliability: Exploring the Effects of Variation and Uncertainty*, 1st ed.; Bergman, B., de Mare, J., Loren, S., Svensson, T., Eds.; John Wiley & Sons Ltd.: West Sussex, UK, 2009; pp. 85–96. ISBN 978-0-470-71394-5.
18. Bergman, B.; de Mare, J.; Loren, S.; Svensson, T. (Eds.) *Robust Design Methodology for Reliability: Exploring the Effects of Variation and Uncertainty*, 1st ed.; John Wiley & Sons Ltd.: West Sussex, UK, 2009; ISBN 978-0-470-71394-5.
19. Johannesson, P. P.; Speckert, M. (Eds.) *Guide to Load Analysis for Durability in Vehicle Engineering*, 1st ed.; John Wiley & Sons Ltd.: West Sussex, UK, 2013; ISBN 978-1-118-64831-5.
20. Svensson, T.; Johannesson, P. Reliability fatigue design, by rigid rules, by magic or by enlightened engineering. *Procedia Eng.* **2013**, *66*, 12–25. [\[CrossRef\]](#)
21. Johannesson, P.; Bergman, B.; Svensson, T.; Arvidsson, M.; Lönnqvist, Å.; Barone, S.; de Maré, J. A robustness approach to reliability. *Qual. Reliab. Engng. Int.* **2013**, *29*, 17–32. [\[CrossRef\]](#)
22. Johannesson, P. (Ed.) Reliability Guidance for Marine Energy Converters. Report RiaSoR (Reliability in a Sea of Risk). December 2016. Available online: http://riator.com/wp-content/uploads/2016/12/ReliabilityGuidanceMECs_v1.0_20161216.pdf (accessed on 18 May 2022).
23. Jia, C.; Ng, C.; McKeever, P.; Johannesson, P.; Svensson, T.; Buck, E.; Shanks, A. Improving reliability in a sea of risk. In Proceedings of the 12th European Wave and Tidal Energy Conference, Cork, Ireland, 27 August–1 September 2017.
24. Johannesson, P.; Svensson, T.; Gaviglio, H. Reliability evaluation using variation mode and effect analysis: Application to CorPower’s mooring pre-tension cylinder. In Proceedings of the 13th European Wave and Tidal Energy Conference, Napoli, Italy, 1–6 September 2019.
25. Yang, S.-H.; Ringsberg, J.W.; Johnson, E.; Hu, Z.Q.; Duan, F.; Bergdahl, L. Experimental and numerical investigation of a taut-moored wave energy converter—A validation of simulated buoy motions. *Proc. Inst. Mech. Eng. Part M J. Engng. Marit. Env.* **2018**, *232*, 97–115. [\[CrossRef\]](#)
26. Yang, S.-H.; Ringsberg, J.W.; Johnson, E. Parametric study of the dynamic motions and mechanical characteristics of power cables for wave energy converters. *J. Mar. Sci. Technol.* **2018**, *23*, 10–29. [\[CrossRef\]](#)
27. Yang, S.-H.; Ringsberg, J.W.; Johnson, E.; Hu, Z.Q. Experimental and numerical investigation of a taut-moored wave energy converter: A validation of simulated mooring line forces. *Ships Offshore Struct.* **2021**, *15* (Suppl. 1), S55–S69. [\[CrossRef\]](#)
28. Ringsberg, J.W.; Yang, S.-H.; Lang, X.; Johnson, E.; Kamf, J. Mooring forces in a floating point-absorbing WEC system—A comparison between full-scale measurements and numerical simulations. *Ships Offshore Struct.* **2021**, *15* (Suppl. 1), S70–S81. [\[CrossRef\]](#)
29. Kuznecovs, A.; Ringsberg, J.W.; Yang, S.-H.; Johnson, E. A methodology for design and fatigue analysis of power cables for wave energy converters. *Int. J. Fatigue* **2019**, *122*, 61–71. [\[CrossRef\]](#)
30. DNV GL. *Subsea Power Cables in Shallow Water*, DNVGL-RP-0360; Det Norske Veritas (DNV): Høvik, Norway, 2016.
31. DNV GL. *Sesam SIMA V3.4-00*; Det Norske Veritas (DNV): Høvik, Norway, 2017.
32. Ishikawa, K.; Loftus, J. *Introduction to Quality Control*; 3A Corporation: Tokyo, Japan, 1990.
33. Lang, X.; Yang, S.-H.; Ringsberg, J.W.; Johnson, E.; Guedes Soares, C.; Rahm, M. Comparison between full-scale measurements and numerical simulations of mooring forces in a floating point-absorber WEC system. In Proceedings of the 3rd International Conference on Renewable Energies Offshore, Lisbon, Portugal, 8–10 October 2018; pp. 865–876.

-
34. Hindrum, K.; Hüffmeier, J. *R&D of Dynamic Low Voltage Cables between the Buoy and Floating Hub in a Marine Energy System*; Report; Swedish Energy Agency: Eskilstuna, Sweden, 2018.
 35. O'Connor, P.; Kleyner, A. *Practical Reliability Engineering*, 5th ed.; John Wiley & Sons: Hoboken, NJ, USA, 2012.